Journal of Structural Geology, Vol. 2, No. 4, 1980, pp. 397 to 410.
Pergamon Press Ltd. 1980. Printed in Great Britain

0191-8141/80/1201-0397 $02.00/0

Extensional structures in anisotropic rocks

J. P. PLATT

Department of Geology and Mineralogy, Oxford University, Parks Road,
Oxford OX1 3PR, England

and

R. L. M. VISSERS

Department of Earth Sciences, University of Utrecht, Budapestlaan 4,
Utrecht-Uithof, The Netherlands

(*Received* 27 *July* 1979; *accepted in revised form* 15 *August* 1980)

Abstract—A distinct class of structures can form as a result of extension along a plane of anisotropy (foliation). The effect of the foliation is to decrease the ductility of the material in this orientation so that brittle fractures or shear-bands develop. Foliation boudinage is caused by brittle failure; extensional fractures cause symmetric boudinage, and shear fractures cause asymmetric boudinage.

Extensional crenulation cleavage is defined by sets of small-scale ductile shear-bands along the limbs of very open microfolds in the foliation. The sense of movement on the shear-bands is such as to cause a component of extension along the older foliation. Conjugate cleavage sets indicate coaxial shortening normal to the foliation; the shortening axis bisects the obtuse angle between the sets. A single set indicates oblique or non-coaxial deformation.

Extensional crenulation cleavage is microstructurally and genetically distinct from other types of cleavage. It does not occur as an axial plane structure in folds, and has no fixed relationship to the finite strain axes. It is common in mylonite zones, and may be favoured by crystal-plastic and cataclastic deformational mechanisms. These cause grain-size reduction, and hence softening, which favour the development of shear-bands.

INTRODUCTION

SMALL-SCALE structures in rocks are commonly controlled by mechanical inhomogeneities (such as bedding) or by anisotropy (cleavage and foliation). The way that layers of differing viscosity control the form of folds, for example, is reasonably well understood (see Hobbs *et al.* 1976 for a review) but the effect of a planar anisotropy is less well known. Current discussion is mainly based on the theoretical work of Biot (1965), who predicted the appearance of perturbations during deformation of anisotropic materials. His conclusions have been extended qualitatively by Cobbold *et al.* (1971) and Cosgrove (1976), who used them to explain structures such as kinks and crenulations in foliated and thinly layered rocks. These authors predict the appearance of a distinct class of structures when the principal extension direction lies close to the plane of anisotropy (foliation). They suggest that pinch-and-swell or boudin-like structures, normal kink-bands, and conjugate crenulation cleavage (Rickard 1961) may form in this way. The purpose of this paper is to document some well-developed natural examples of such structures, and to discuss some ideas on their genesis.

FOLIATION BOUDINAGE

Hambrey & Milnes (1975) describe a structure resembling boudinage in glacier ice. They suggest that it is controlled by the presence of a pre-existing foliation, and refer to it as 'foliation-boudinage'. We have found similar structures in strongly foliated quartzo-feldspathic schists forming part of an Archaean metasedimentary sequence near Agnew, Western Australia. Deformation took place in a 1 km wide NNE trending dextral shear zone (Waronga shear zone), which produced an intense vertical foliation (trend 010°) and a subhorizontal elongation lineation (Platt *et al.* 1978). The schist forms a layer about 10 m thick, within which no significant compositional or textural variation is apparent in outcrop or in thin-section. The rock consists mainly of quartz (30–40%) and sodic plagioclase (50–60%), occurring as monomineralic lenticles about 100 μm thick, which define the principal foliation. The lenticles have been recrystallized to aggregates of 100 μm grains that are largely free of lattice distortion. Up to 15% of mica occurs as flakes parallel to the foliation. This deformational fabric is vertical and trends at about 010°, parallel to the lithologic layering and to the shear zone.

A weak secondary cleavage is also present; this is an extensional crenulation cleavage of the type described later in this paper. The cleavage zones, which displace the principal foliation, are short (1–2 mm), and are spaced at about 2 mm intervals. They may be marked by a 20 μm thick film of biotite. The cleavage is vertical, and trends about 040°. (The principal foliation and the secondary cleavage are visible in Figs. 5c & d.) The principal foliation is regionally planar and undeformed. Foliation boudinage occurs on the scale of a few centimetres (Figs. 1 and 5) and may be symmetric or asymmetric.

Symmetric boudinage

These are small-scale pull-apart structures defined by

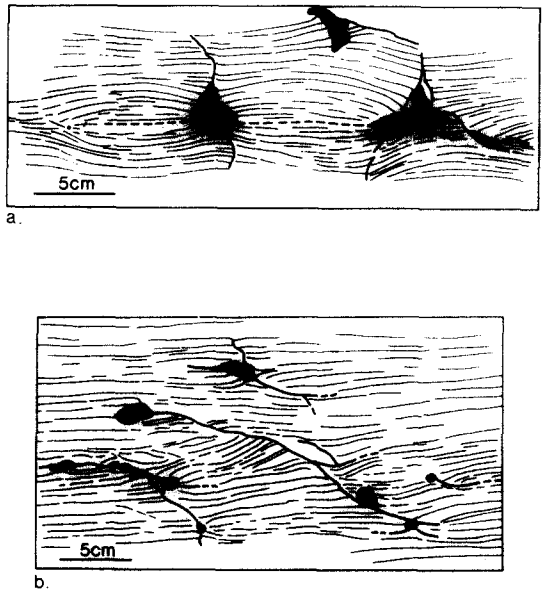

Fig. 1. Foliation boudinage, Waronga shear zone. Surfaces are horizontal. (See also Figs. 5a & b.) Light lines: foliation traces. Heavy lines: fractures. Black: quartz veins. (a) Symmetric. Note quartz-filled extension fractures at high angles to foliation (S). (b) Asymmetric. Note low angle dextral fractures, and reverse drag, particularly in centre. Outcrop 4.9 km at 255° from Agnew, Western Australia (28° 01'S, 120° 28'E).

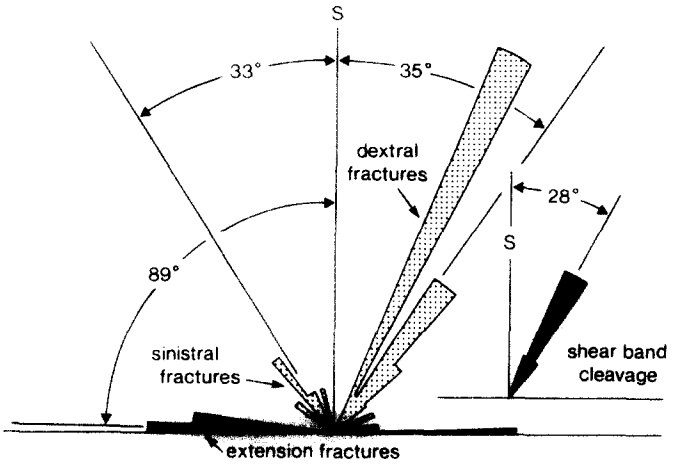

Fig. 2. Trends of fractures associated with foliation boudinage. S: principal foliation trend. The trend of the shear-band cleavage in the same outcrop is also shown. All surfaces are nearly vertical. Mean orientations, measured clockwise from S, are as follows: dextral fractures: 34.8° (σ:10.1°, n:22); sinistral fractures: 32.8° (σ:11.6, n:7); extensional fractures: 91.1° (σ:5.1°, n:8); shear-band cleavage: 28.1° (σ:5.1°, n:8).

fractures, roughly normal to the foliation, that have been opened out into diamond shapes by differential extension along the foliation (S) (Figs. 1a and 5a). The foliation around the fracture is pinched in towards the resulting void, so that the structures resemble boudins. The voids are now filled by coarse (2 mm) quartz and white mica, which show no signs of internal deformation. In some cases fragments of schist have been broken off and rotated (Fig. 5c). The principal foliation is well-developed in these fragments, indicating that it was present prior to the onset of boudinage. The structures differ from classical boudins in that they do not occur in trains and are not associated with any obvious compositional contrasts in the rock.

Asymmetric boudinage

Closely related structures develop where the rock has broken along surfaces oblique to the foliation (Figs. 1b and 5b & d). The displacement in these cases is roughly parallel to the fracture, so that quartz-filled voids do not generally form. The sense of displacement is always such as to cause a component of extension along the foliation. The fractures curve at each end towards the foliation, where the displacement diminishes, apparently to zero. The most distinctive feature is that the foliation curves as it approaches the microfault in a sense opposite to the sense of displacement on the fault (Figs. 1b and 5b). This 'reverse drag' effect (Hobbs *et al.* 1976) produces the boudin-like geometry. Ordinary drag effects also occur. Some fracture zones contain rotated angular fragments of schist or patches of microbreccia. This, and the lack of concentrations of insoluble residues along them, indicate that they are not solution surfaces.

Both NE trending (dextral) and NW trending (sinistral) fractures are developed (Fig. 2). The dextral fractures form a complex anastomosing pattern; both asymmetric and symmetric pinch-ins, and irregular quartz-filled voids may be distributed along them (Figs. 1b and 5b). In places they occur in sets spaced at intervals of about 5–10 cm.

The dextral fracture set is roughly parallel to the extensional crenulation cleavage in the same outcrop (Fig. 2). The two features also have similar geometries; the cleavage being defined by a set of small-scale ductile shear zones with the same sense of displacement as the dextral fractures. It is likely that the ductile extension parallel to the foliation that accompanied boudinage was achieved by formation of the crenulation cleavage.

Origin of foliation boudinage

Ordinary boudinage results from a difference in ductility between a competent layer and its matrix. In these examples, however, there is no compositional layering on a scale comparable to that of the boudins. The strong planar anisotropy caused by the foliation may, therefore, have caused the boudinage.

Cobbold *et al.* (1971) applied Biot's (1965) analysis of deformational instabilities in anisotropic materials to the condition of shortening normal to the foliation, and predicted the formation of symmetric pinch-and-swell structures. The analysis is limited to infinitesimal deformations however, and does not predict brittle failure. As fracture appears essential to these structures we suggest the following alternative.

The presence of a strong foliation limits the rate of ductile extension parallel to S. Extensional fractures form normal to S (Fig. 3a) and open out along S (Fig. 3b). The open fractures and the adjacent foliation are then pinched

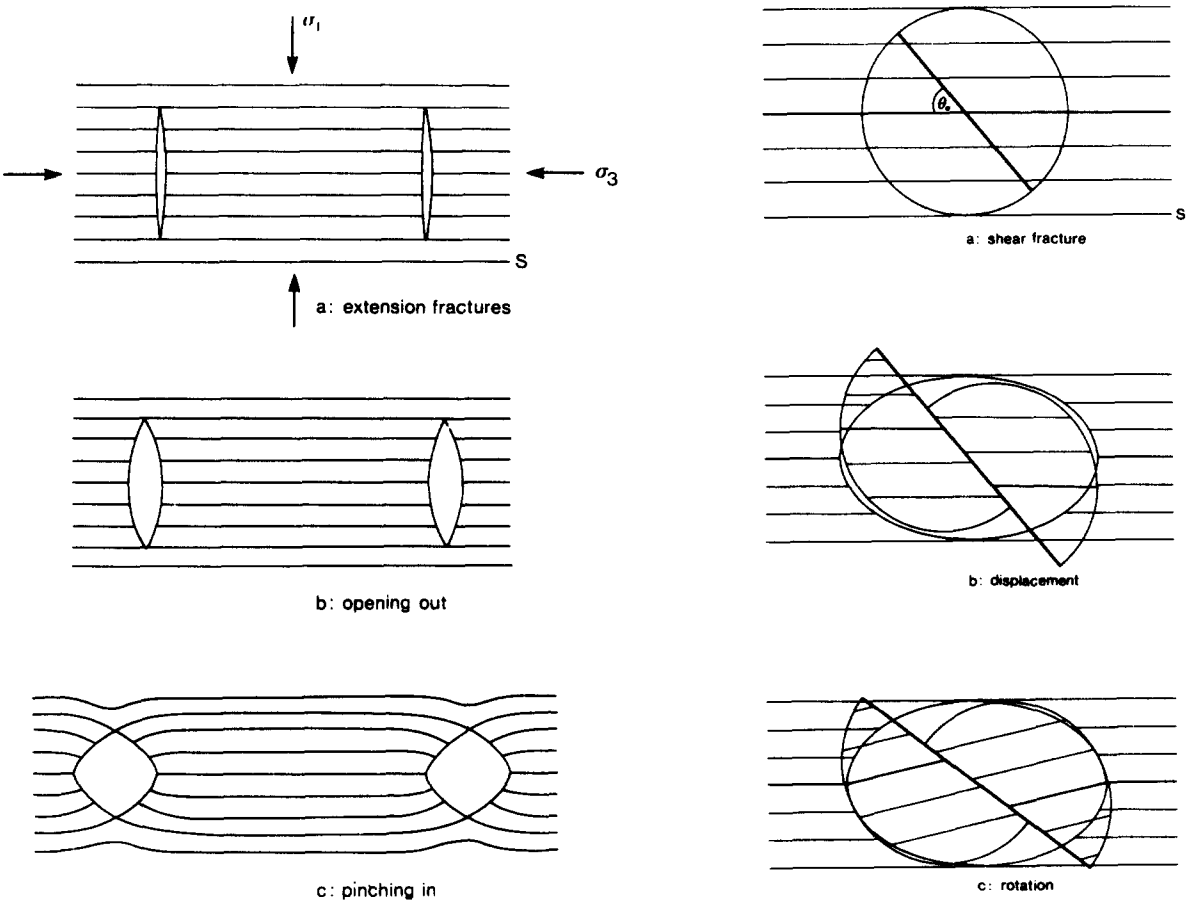

Fig. 3. Origin of symmetric foliation boudinage. See text for discussion.

in by shortening normal to S (Fig. 3c). This implies that the finite pinch-and-swell geometry was caused by, and followed, brittle failure.

The asymmetric boudins are closely associated with the symmetric structures, and the two types probably formed under similar conditions. They are caused by shear fractures, rather than extension fractures, but the sense of displacement along both sets of shear fractures is such as to cause extension along S. The apparent pinching in of the foliation (reverse drag) results from rigid-body rotation of both the fracture and the foliation adjacent to it, in compensation for slip on the fracture. This is illustrated sequentially in Fig. 4. We assume that shear failure, by relieving the stress field, inhibits ductile deformation in the immediate surroundings (shown as a circle in Fig. 4a). While the material as a whole undergoes continuous ductile shortening normal to the foliation, the body of rock adjacent to the fracture deforms only by slip along the fracture (Fig. 4b). A compensatory rotation (Fig. 4c), and second-order distortions (Fig. 4d) are required to maintain continuity. These processes occur continuously and simultaneously. They are discussed further in Appendices A–C.

The dextral and sinistral fractures sets (Fig. 2) form a dihedral angle of approximately 110° about the probable orientation of the bulk shortening direction. Shear failure criteria (Murrell 1977) generally predict dihedral angles of

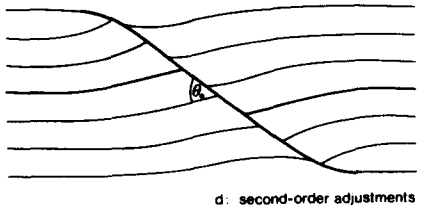

Fig. 4. Origin of asymmetric foliation boudinage. See text for discussion.

60–80°, and always less than 90°. The model outlined above, however, predicts that both types of fracture will rotate towards the enveloping surface of the foliation during continued deformation (Appendix B), thereby increasing the dihedral angle. About 35% shortening (plane strain) normal to the foliation would be required to increase the dihedral angle from 60 to 110°. The model also suggests that the angle θ, between the fracture and the foliation abutting it, approximates to the initial angle of fracture (Fig. 4). Available measurements indicate that the initial dihedral angle was 50–80°.

Effect of the foliation

The principal effect of the foliation in controlling these structures is that it causes a variation in ductility with orientation, so that the rock tends to break under

extension at a high angle to the foliation. Oblique deformation would probably cause folding.

After failure, a perturbation in the continuous deformation field is caused by stress relief around the fracture, and by slip along it. This perturbation will arise whether or not the material is anisotropic, although the anisotropy will influence its nature. The foliation, however, acts as a marker, rendering the perturbation visible as boudinage. Similar structures could form in an isotropic material of limited ductility, but in the absence of marker lines, only the fractures would be visible. In essence, the structures are simply perturbations in the ductile deformation field around fractures.

EXTENSIONAL CRENULATION CLEAVAGE

Secondary spaced cleavages can form in foliated materials extended in the plane of the foliation. Muff (in Peach *et al.* 1909), Knill (1959), Rickard (1961), and Williams (1979) describe conjugate sets of crenulation cleavages symmetrically disposed about an earlier slaty cleavage, and suggest that they were caused by shortening normal to the older cleavage, possibly in the course of a continuing coaxial deformation. Means & Williams (1972) produced analogous structures by shortening salt-mica aggregates normal to the foliation. These authors all suggested that the cleavage zones are either microfaults or small-scale ductile shear zones formed symmetrically about the maximum shortening direction. This tied in with the widely held idea that crenulation cleavage in general represents sets of microfaults or shear zones [for reviews see Turner & Weiss (1963) and Ramsay (1967)].

Recent workers have attributed crenulation cleavage to small-scale folding of an earlier foliation [internal buckling in the sense of Biot (1965)] caused by a component of shortening along the foliation. Microfolding is accompanied by diffusion of material (mainly quartz) from the limbs to the hinges of microfolds (Cosgrove 1976, Fletcher 1977, Marlow & Etheridge 1977). Concentrations of insoluble minerals (such as micas) remain in the limb zones and define the new cleavage. Offsets across the cleavage zones can be explained by volume reduction within the zones, rather than by shear along them [but see Williams (1976)].

Cobbold *et al.* (1971) and Cosgrove (1976) suggested that a type of internal buckling might also be caused by extension along the foliation, and that the perturbations predicted by Biot might amplify in this situation into conjugate sets of 'normal' (that is extensional) kink-bands, or into conjugate crenulation cleavage. Here we describe natural examples of single, multiple, and conjugate sets of crenulation cleavages apparently formed during extension along an earlier foliation. We present pertinent information on the tectonic setting and on the cleavage microstructure.

The Betic Movement Zone

Our best examples come from a major zone of intense ductile deformation developed beneath the Alpujarride nappe complex in the Betic Cordilleras of southern Spain (Torres-Roldán 1979). Upper greenschist to amphibolite facies schist has undergone intense deformation and retrograde metamorphism in a zone a few tens to several hundreds of metres thick beneath the basal contact of the nappe. The schist has an intense platy foliation produced by isoclinal folding, transposition, and modification of pre-existing layering and schistosity. Deformational mechanisms were dominantly crystal-plastic and cataclastic. Quartz has a strong grain-shape fabric (grain-size 100–200 μm), and lattice preferred orientation; original coarse-grained (> 1 mm) white mica has been deformed and recrystallized to interleaving aggregates of 100–200 μm grains; feldspar has been broken and forms augen in the foliation. Intercrystalline diffusion was minimal: no chemical differentiation occurred, and mineral growth was limited to retrogressive alteration of garnet, staurolite and biotite to chlorite. Oriented minerals and grain aggregates define a strong N–S elongation lineation, subparallel to the isoclinal fold axes.

The principal foliation is commonly affected by a distinctive type of weak crenulation cleavage, best developed in micaceous rock-types. The main characteristics of the cleavage are illustrated in Figs. 6, 7 and 9, and

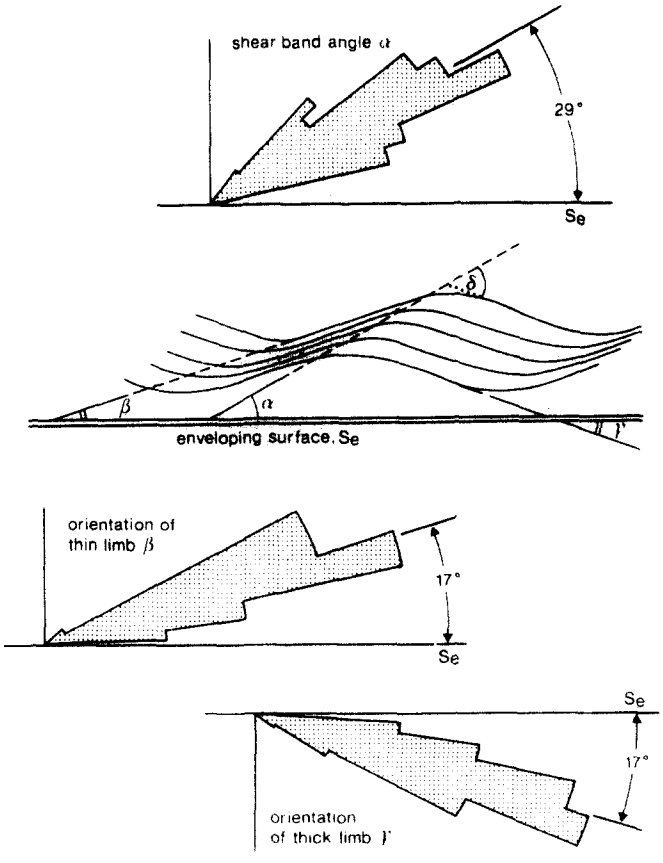

Fig. 9. Geometry of extensional crenulation cleavage, Betic Movement Zone. Angles are measured with respect to the enveloping surface of the principal foliation (Se). Mean values are: $\alpha - 29.4°$ (σ:9.3°, n:75); $\beta - 16.8°$ (σ:7.9°, n:65); $\gamma - 16.9°$ (σ:7.5°, n:67); $\delta - 47.4°$ (σ:11.54, n:53).

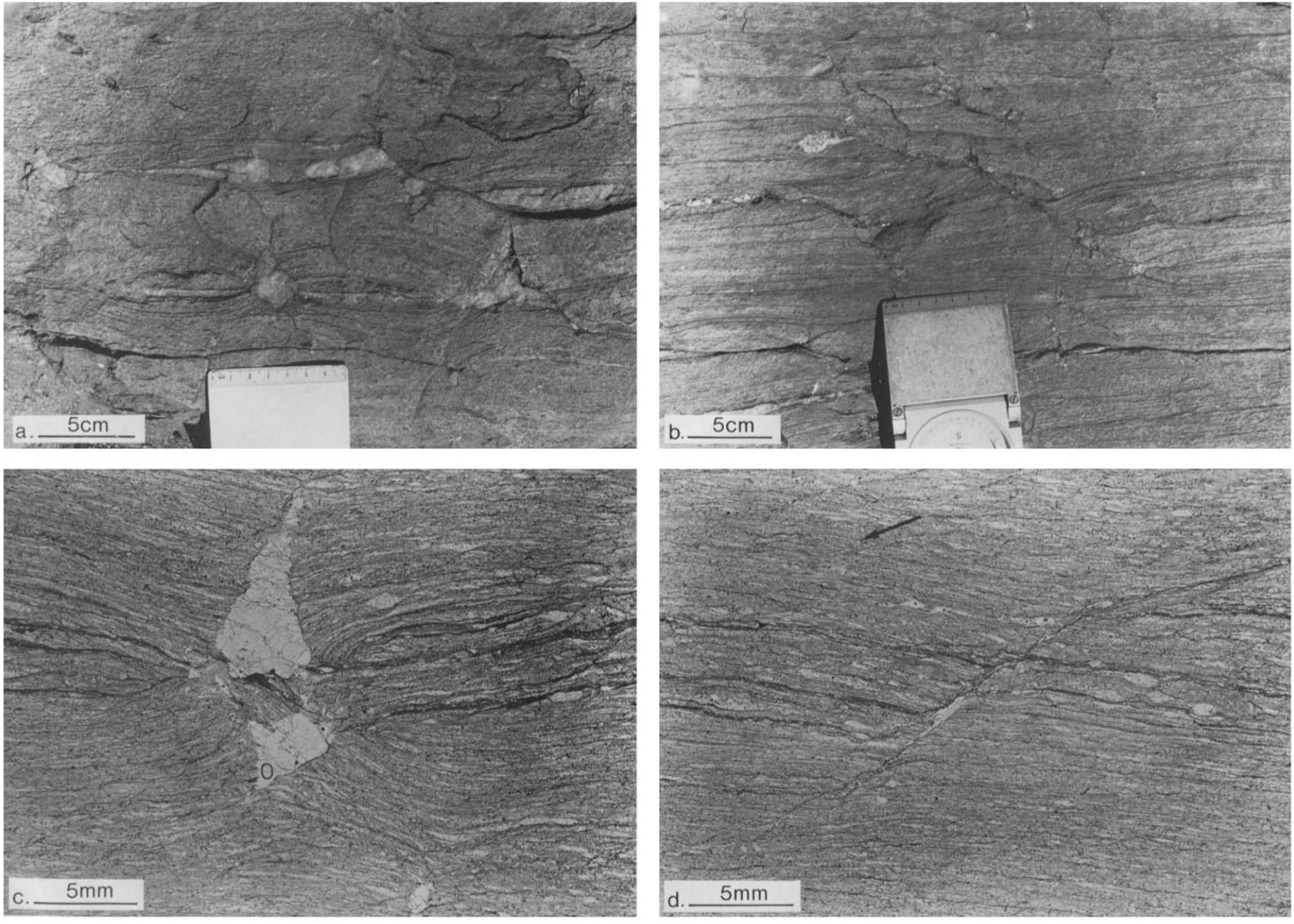

Fig. 5. Foliation boudinage, Waronga shear zone, Western Australia. (a) Field example of symmetric boudinage (see also Fig. 1a). (b) Field example of asymmetric boudinage (see also Fig. 1b). (c) Photomicrograph of symmetric boudinage. Note the rotated schist fragment inside the quartz-filled extension fracture. (d) Photomicrograph of asymmetric boudinage. Note the weak shear-band cleavage (arrow).

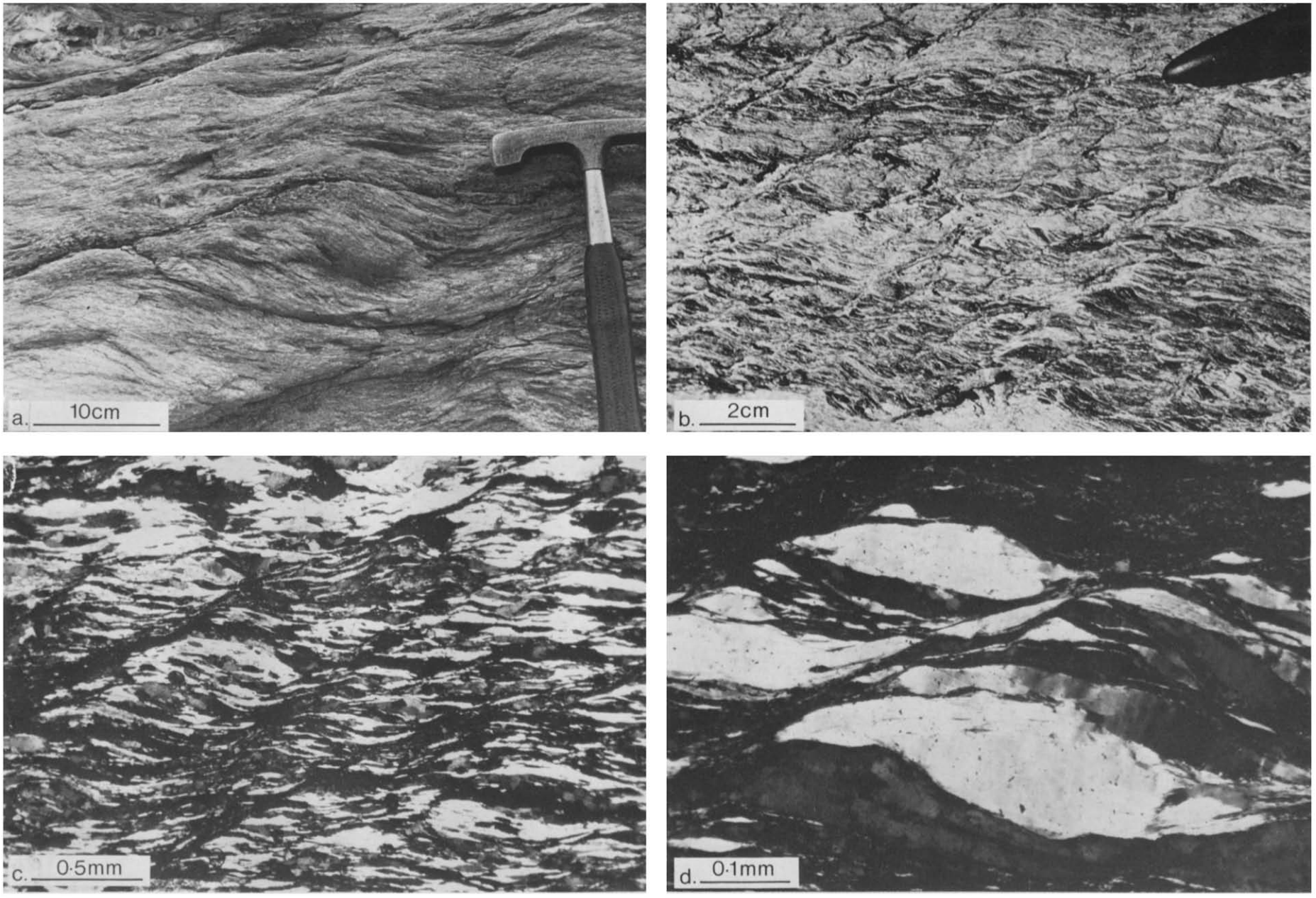

Fig. 6. Extensional crenulation cleavage. (a) Phyllite in shear zone below the Glacier de l'Arpont, 5.5 km at 308° from Termignon, Vanoise massif, French Alps. Cleavage spacing about 15 cm. (b) Mylonitic schist, Sierra Alhamilla, southeast Spain (583973 on Tabernas 1:50 000 sheet 23–42). Spacing 1–2 cm. (c) Photomicrograph of mylonitic schist (Pt 265), Sierra de los Filabres, southeast Spain (494035). Spacing 0.5–1 mm. (d) Detail of cleavage structure in mylonitic schist (Pt 460), Sierra Alhamilla (615936).

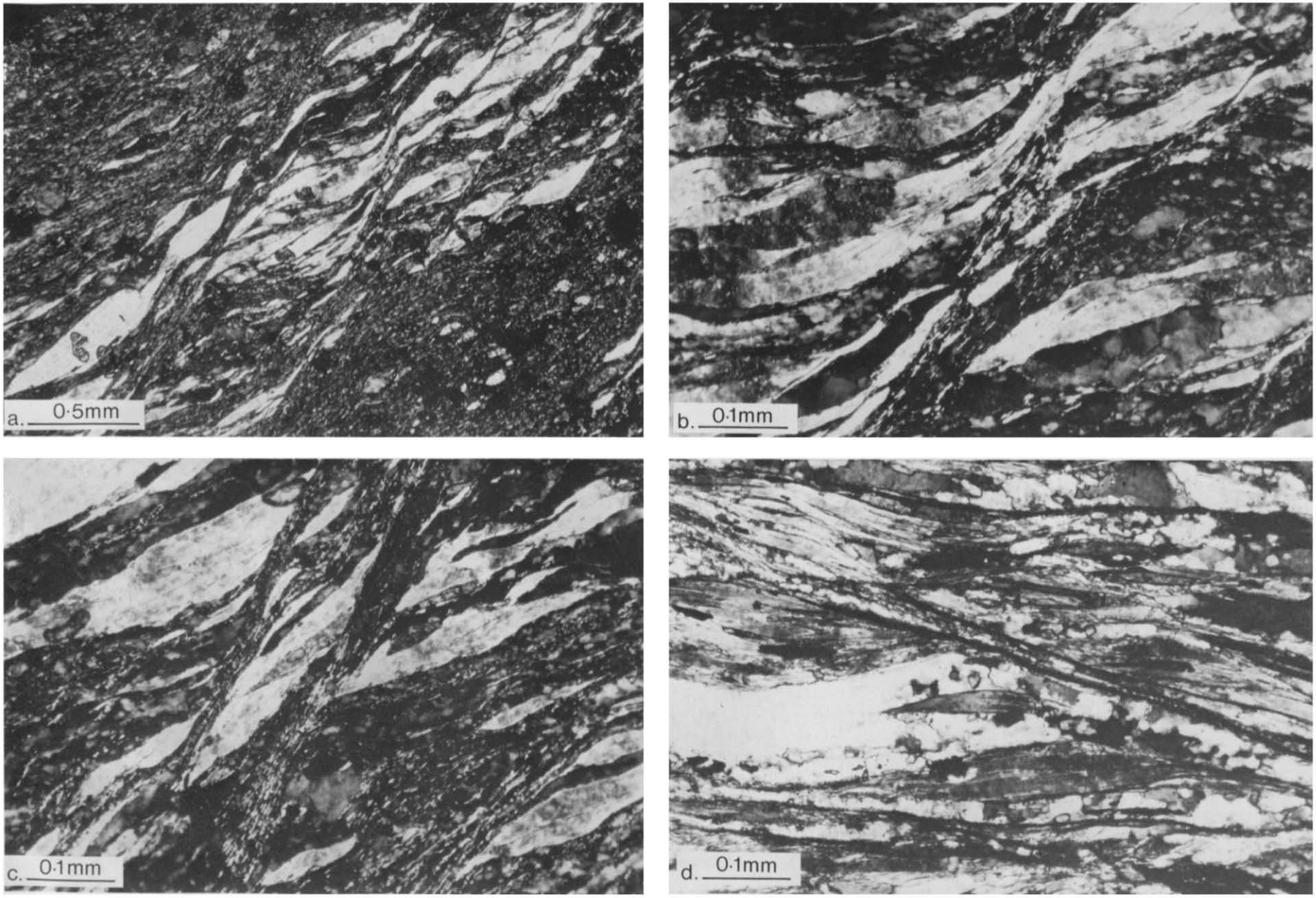

Fig. 7. Cleavage microstructure. (a) Overview of cleavage in mylonitic schist (Pt 460). Note that there is no obvious concentration of mica in the cleavage zones. (b) Detail of cleavage zone at centre of Fig. 7(a). Note bending and internal deformation of mica, and very fine-grained white mica in the cleavage zone. (c) Detail from bottom left of Fig. 7(a). Note abrupt truncation of mica grains at the margin of the cleavage zone. (d) Variation in quartz microstructure adjacent to a shear-band in mylonitic schist, Sierra de los Filabres.

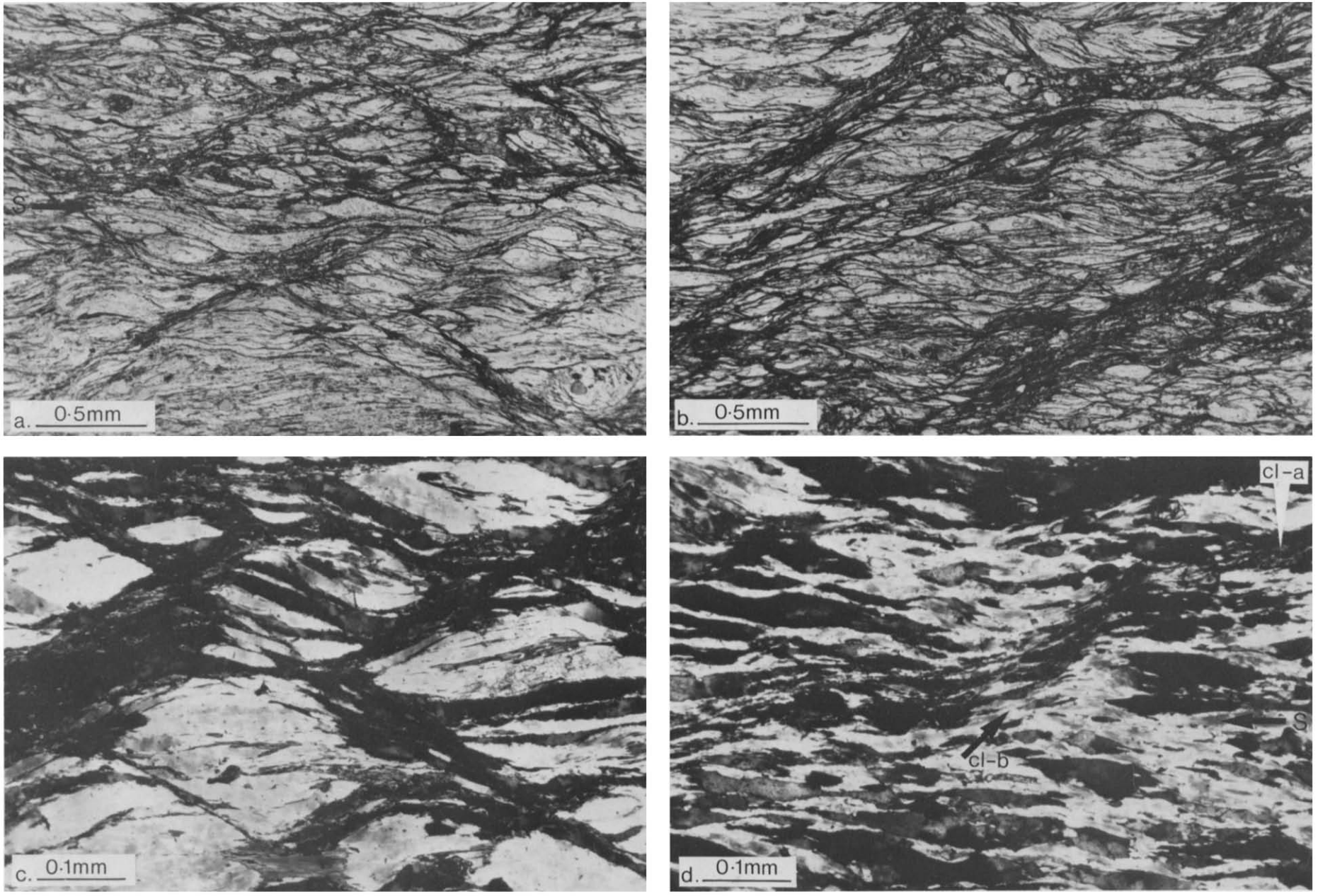

Fig. 8. Conjugate and multiple sets. (a) Intersecting conjugate sets of cleavages, in mylonitic schist (Pt 458), Sierra Alhamilla (615935). Mylonitic foliation (S) is marked by ribbon quartz. Plane light. (b) Broadly spaced dominant set dips left (spacing 1–2 mm). Weaker conjugate set (spacing 0.1–0.2 mm) dips right in the microlithons of the dominant set. (c) Intersecting conjugate sets. Note chlorite-filled pull-apart (bottom centre). (d) Old low-angle cleavage zone (cl-a), defined by a narrow fine-grained zone clearly oblique to the schistosity (S), is warped by open crenulations. These are beginning to define a new, high-angle, cleavage (cl-b). Pt 265.

are summarized below.

(1) The foliation (S) is affected by very open, approximately symmetric, microfolds. The limbs are inclined at only 10–25° to the enveloping surface of the folded S, and the apical angle generally exceeds 130°.

(2) One set of limbs is much thinner than the other. The thinner limbs are zones of high deformation intensity and define the spaced cleavage. The cleavage zones are generally inclined at 20–40° to the enveloping surface, and at 50–70° to the bisector of the microfold limbs. They appear to displace S, and continuity may be lost across them.

(3) The apparent sense of displacement on the cleavage zones is always such as to cause a component of extension along S.

(4) The cleavage zones are discontinuous and anastomosing, and they tend to curve into and merge with S. The length of an individual zone is commonly not much greater than the wavelength of the crenulations.

(5) The intersection of the cleavage with S is rarely clearly visible, and is commonly non-linear. This suggests that the cleavage zones are non-planar and discontinuous. Where the cleavage is strongly developed, the older S-surfaces have an irregular, 'fish-scale' or 'button-schist' appearance.

The cleavage zones are rarely strong enough to create a new splitting surface, so that the structure is not a true cleavage in the sense of a plane of fissility. This makes systematic field measurement difficult, particularly where more than one set is developed. The spacing is usually between 1 mm and 2 cm, but similar structures are locally developed on scales up to several metres.

In thin-section the cleavage zones are clearly distinguishable as zones of intense microstructural modification. Mica in the microlithons between cleavage zones has a grain size of 100–200 μm: this is reduced to less than 5 μm locally within the zone (Fig. 7c). Near the cleavage zones, mica grains are bent and broken along internal fractures at low angles to the basal plane. At the zone boundaries, the mica grains either curve into the zone (Fig. 7d), or are cut off by discrete microfaults (Fig. 7c). Subgrain structure in quartz is more noticeable near the cleavage zones (Fig. 7d), and within the zone dynamic recrystallization has reduced the grain-size to less than 5 μm. The other main constituent of the cleavage zones is chlorite, in the form of minute (<5 μm) flakes. This was probably produced in part by retrogressive breakdown of higher grade Fe–Mg minerals, and indicates a limited degree of diffusion and metamorphic reaction during deformation. There is no marked change in bulk composition within the cleavage zones: however the proportions of quartz, white mica, and Fe–Mg minerals appear to be about the same as in the rock as a whole.

Nature of the cleavage zones

It is important to establish whether volume was conserved during deformation. If volume was lost in the zones (P-zones in the sense of Cobbold 1977a) offsets of the foliation across them would not necessarily be a result of shear along the zones (Groshong 1975). If volume was conserved, the displacements are real, and the zones are microshear-bands (S-zones). Volume changes require diffusion of the solid-phase components. At low temperatures (probably less than 400°C in this case), diffusion is probably assisted by volatile phases. This process (pressure-solution) operates at very different rates in different minerals, and generally causes a marked chemical differentiation (Williams 1972, Gray 1978, Marlow & Etheridge 1977). The lack of chemical differentiation in the cleavage zones probably indicates that volume was approximately conserved, and hence that the zones are microscale shear-bands. The displacements on the cleavage zones are real, therefore; and the deformation has caused significant extension along the older foliation. In our examples, these displacements alone have caused about 50% elongation along S.

Conjugate sets

Two sets of cleavage zones, with opposite senses of displacement, are locally developed (Fig. 8). In effect, both limbs of the open microfolds become the loci of cleavage zones, which intersect with each other to produce an augen or phacoid texture. The two sets are oriented at about 30° on either side of S. Commonly, the two sets are unequally developed. The weaker set may be developed on a smaller scale within the microlithons separating the cleavage zones of the dominant set (Fig. 8b).

Multiple sets

In some very micaceous schists, consistent overprinting relations indicate that two or more sets of cleavages with the same sense of displacement are present: cleavage zones at a low angle to S are offset and crenulated by younger zones at a higher angle (Figs. 8d and 10). Similarity in styles, spacing, and microstructural development of the different sets suggest that they developed sequentially during a single progressive deformation. As

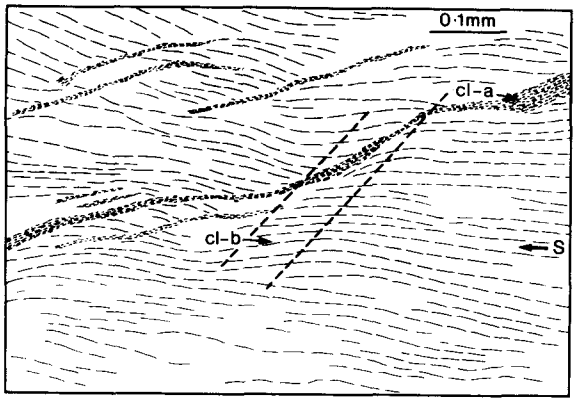

Fig. 10. Overprinting of cleavage sets in quartz–muscovite schist (Pt 265): interpretative sketch from Fig. 8(d). S:-principal schistosity. cl-a: fine-grained zones defining the older extensional crenulation cleavage. cl-b: incipient new cleavage zone defined by thinner limb of younger crenulation.

discussed below, cleavage zones rotate towards the enveloping surface of S during progressive deformation. Our observations suggest that after a certain amount of strain, new zones initiate at a higher angle to S.

Tectonic relationships

The Betic Movement Zone is spatially related to the base of the Alpujarride nappe, which can be shown on structural grounds to have been emplaced towards the north. We believe the extensional crenulation is genetically related to nappe emplacement and mylonization for the following reasons. (a) The cleavages are only developed within the zone of mylonitic deformation. (b) They predate all other post-mylonite folding events. (c) Deformational mechanisms were similar during the formation of the principal foliation and the crenulation cleavages; the latter contribute significantly to the mylonitic aspect of the rocks. There is however, no clear-cut relationship between the sense of displacement on the shear-bands and the sense of transport of the nappe: conjugate cleavages sets and alternating sets of opposite displacement are common.

Vanoise Massif, French Alps

Extensional crenulation cleavages are widely developed in schists of the Vanoise Massif in the French Penninic Alps (Platt & Lister 1978). They are particularly strong in zones of quartz–phengite phyllite developed along shear zones, where they are typically spaced on a 2–20 cm scale (Fig. 6a). Conjugate sets are developed, but a subhorizontal set with a 'top side to east' sense of displacement is dominant. These phyllitic movement zones formed early in the tectonic history of the area, during the main phase of nappe emplacement. The extensional crenulation cleavage is much younger, and appears to be associated with a late phase of large-scale southeast-directed folding and thrusting in the area.

Waronga shear zone

The extensional crenulation cleavage already described from the Waronga shear zone is restricted to the zone, and immediately post-dates mylonitic deformation. The sense of displacement on the cleavage zones is the same (dextral) as on the major shear zone. The cleavage zones are oriented about 20° clockwise from the boundaries of the shear zone.

Origin of extensional crenulation cleavages

In all three areas from which we have described extensional crenulation cleavage, the rocks are homogeneous at the scale of the cleavage. Hence the microfolding cannot be explained by buckle-folding of layers of contrasting effective viscosity. All the rocks have a strong pre-existing plane of anisotropy, and it appears to be this feature which controlled the development of the new cleavage.

The initial perturbations that lead to these structures may be explained, as Cobbold *et al.* (1971) and Cosgrove (1967) suggest, by Biot's (1965) theory for anisotropic materials. The theory only deals with infinitesimal deformations, however: here we consider the problem of amplification.

Our microstructural evidence indicates that the cleavage zones are microscale shear-bands. The development of a shear-band in an initially homogeneous material requires that the material in the zone becomes more deformable (softer) than the material outside it (Ramsay & Graham 1970). The following possible causes of rheological change during deformation can be distinguished (Cobbold 1977b, Poirier 1980).

(a) Temperature change.
(b) Strain or strain-rate sensitivity of the deformation mechanisms.
(c) Rotation of a plane of anisotropy with respect to the stress field.
(d) Microstructural change induced by deformation.

Temperature change is unlikely to be significant on the scale of individual cleavage zones. Strain and strain-rate sensitivities of individual deformational mechanisms generally lead to hardening, except for temporary stress-drops associated with plastic yield in metals (Poirier 1980). Rotation of the plane of anisotropy in a foliated material can have a marked softening effect; this may be a principal cause of folding in anisotropic materials (Cobbold 1976a, b). If the foliation is initially normal or parallel to the maximum principal stress, any rotation will lead to a component of shear stress along the foliation in the perturbed domain. The material deforms more easily in the new orientation and hence it becomes effectively softer. Whether or not such a rotational perturbation will amplify depends on the relative vorticities inside and outside the perturbation (Appendix B). For shortening normal to S the vortical component of flow within the perturbation will be larger than that outside it, and will be in the same sense as the initial rotation. It must be compensated for by a spin component in the opposite sense, which will reduce the amplitude of the perturbation.

Changes in the microstructure of the deforming material may profoundly influence its rheology. In particular, deformational mechanisms for which diffusion to or from grain-boundaries is the rate-controlling step are greatly aided by grain-size reduction (Nicolas & Poirier 1976, Boullier & Gueguen 1975). Softening caused by grain-size reduction has been suggested as a reason for shear zone development by Watterson (1975), White (1976), and Cobbold (1977b). In view of the marked decrease in grain-size in the cleavage zones, we suggest that they were caused by this type of microstructural softening. Grain-size reduction was probably caused by dynamic recrystallization and by cataclasis; softening, however, may have involved increased activity of diffusional mechanisms of deformation. Disruption of the foliation in the shear-bands will also contribute a significant softening effect, as it weakens the anisotropy.

Orientation of the shear-bands

The boundaries of a discrete shear-band are likely to be discontinuities in the rate of shear strain. At scales on which the material can be treated as a continuum, shear-bands are likely to propagate along the characteristic directions of the flow field (Odé 1960). For isotropic solids obeying a plastic yield criterion independent of confining pressure, these are parallel to the directions of maximum shear stress and maximum rate of shear strain (Hill 1950). This may also be true for anisotropic materials symmetrically oriented in the stress field. In asymmetrically oriented anisotropic materials, stress and strain rate axes are not parallel. We assume here that shear-bands will propagate along surfaces close to the directions of maximum rate of shear strain.

If microstructural softening occurs, the shear-bands will develop into finite structures, but they will become fixed parallel to material planes. These will in general rotate towards the axis of maximum rate of elongation (D_1) during progressive deformation. As a result, the material as a whole will have to undergo a progressively larger rate of stretching parallel to the bands, and the proportion of the total deformation that can be taken up in the bands becomes progressively smaller. Eventually, they become inactive, and new bands may initiate at about 45° to D_1. This point is discussed further in Appendix D. To determine the relationship of the shear-bands to S_1 we examine some specific situations.

Symmetric coaxial deformation. If we assume coaxial deformation with D_1 parallel to the foliation (S), shear-bands can initiate in two conjugate sets at 45° on either side of S (Fig. 11a). Simultaneous activity on both sets will be difficult: they will probably have to alternate, or operate on different scales. Both sets will rotate with progressive deformation towards D_1, and hence towards the enveloping surface of the foliation (S_e). The dihedral angle formed by the bands about the shortening direction thus becomes greater than 90°.

Asymmetric coaxial deformation. If D_1 is oblique to S, the shear-bands will be asymmetrically oriented about S (Fig. 11b). S is so oriented relative to D_1 that it will tend to deform by slip opposite in sense to slip on the high-angle set of shear-bands. This is consistent with the deformation required for continued activity on the high-angle set as it rotates towards D_1. Activity on the low-angle set would require slip on S in the wrong sense. The high-angle set will therefore be favoured, but it will rotate towards D_1 with progressive deformation.

Non-coaxial deformation. If the imposed deformation is non-coaxial the shear-bands will rotate at different rates towards D_1. The band that rotates more slowly will be able to remain active longer, and will dominate. A simple example is shown in Fig. 11(c). A bulk simple shear at rate Γ is imposed at 45-η to the foliation, giving a maximum stretching axis at η to S, and a bulk vorticity of $\frac{1}{2}\Gamma$ clockwise. The high-angle shear-bands will rotate at Γ clockwise relative to D_1, and must rapidly become inactive. The low-angle set will not rotate at all, and can remain active indefinitely. S_e will rotate towards the low-angle shear-bands. No deformation occurs in the microlithons, so that the angle between the bands and the foliation in the microlithons (S_i) remains unchanged. The prediction for this special case is therefore a single set of bands parallel to the bulk shear direction.

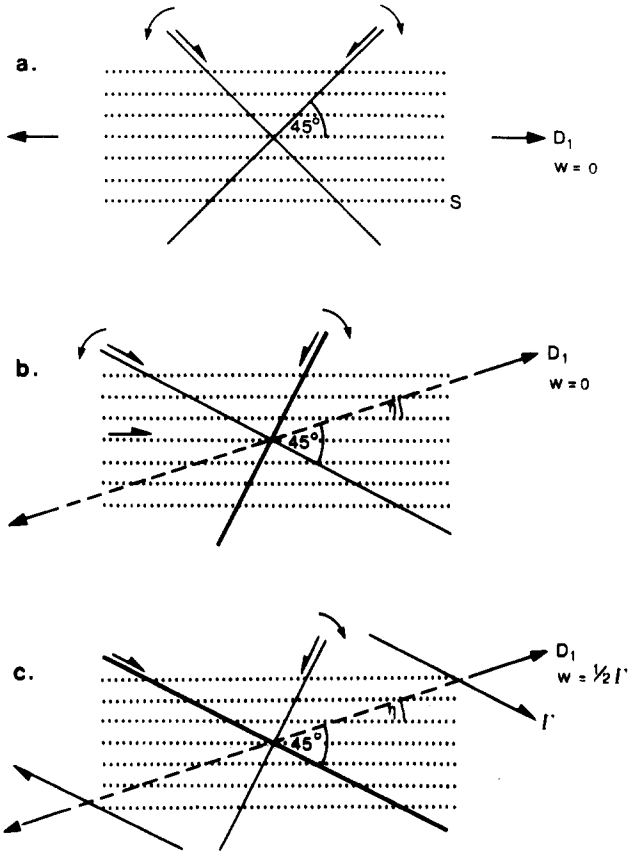

Fig. 11. Orientation of shear-bands. (a) Coaxial deformation, with D_1 parallel to the foliation. The sense of rotation of the shear-bands is shown by the curved arrows. (b) Coaxial deformation with D_1 at η to foliation. The sense of possible associated slip on the foliation is shown. (c) Simple shear at rate Γ at (45-η) to foliation. In (b) and (c) the shear-band shown with the thicker line will be dominant.

Cause of the microfolding

The microfolds are caused by the rotation of the microlithons with their included S_i relative to S_e. This is a geometric consequence of simple shear on the cleavage zones (Appendix D, Fig. 12). The curviplanar form of S is a result of the gradational change in shear strain at the margins of the shear-bands. Note that the microfolds cannot be distinguished geometrically from those produced by other mechanisms. Our interpretation is based on microstructural evidence for volume conservation in the cleavage zones.

Conditions required for cleavage formation

We suggest that extensional crenulation cleavages form in materials shortened at a high angle to a pre-existing foliation. The foliation gives the material high strength in

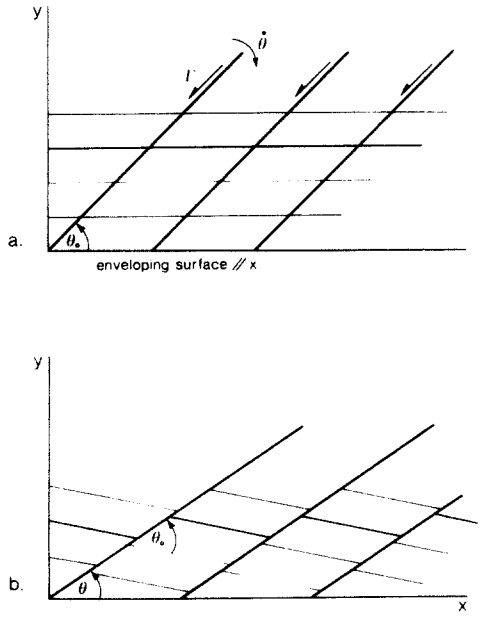

Fig. 12. Kinematics of closely spaced faults or shear-bands: (a) Before movement. (b) After movement. The X-axis is fixed parallel to the enveloping surface of the marker lines. See text for discussion.

this orientation. Another condition is that the material becomes softer when deformed, so that shear-bands initiate. Microstructural softening is likely if deformational mechanisms that cause grain-size reduction, such as dislocation creep and cataclasis, are active. This may explain why extensional crenulation cleavages are common in mylonite zones. Large progressive deformations will favour their formation, as the material develops a strong foliation lying in the extensional sector of the flow field.

Shear-bands can also develop in isotropic materials that soften during deformation. Escher *et al.* (1975) and Berthé *et al.* (1979) describe spaced sets of shear-bands in initially isotropic rocks defining a shear-band cleavage analogous to that described here. The main differences are: (a) shear-band formation is independent of the orientation of the material; and (b) in the absence of an older foliation to act as a marker, the crenulation effect is not developed.

DISCUSSION AND CONCLUSIONS

Rocks with a strong foliation are relatively strong when shortened normal to S. Localized deformation may modify the fabric, weaken the material, and cause yield. Limited brittle failure causes foliation boudinage, which may be symmetric (extension fractures) or asymmetric (shear fractures). Ductile deformational mechanisms, if they cause grain-size reduction, may lead to microstructural softening; this favours development of shear-bands, which define extensional crenulation cleavage. This is common in mylonite zones, and is favoured by large progressive deformations that produce a primary foliation lying in the extensional sector of the flow field.

Extensional crenulation cleavage does not appear to form as an axial plane cleavage in folds. It is genetically distinct from other types of crenulation cleavage, and can be distinguished on the following microstructural grounds: (a) lack of significant chemical differentiation between cleavage zones and microlithons; and (b) textural evidence for approximately constant-volume deformation mechanisms, such as dislocation glide and creep.

Cleavage orientation is not directly related to the axes of finite strain. The shear-bands probably propagate along directions of high rate of shear strain, and then rotate with progressive deformation. They may ultimately become inactive, and new sets may form in a more favourable orientation.

Conjugate sets of extensional crenulation cleavages probably indicate coaxial shortening normal to the older S. Single sets may indicate asymmetric, possibly non-coaxial, deformation. We suggest that in zones of bulk simple shear, a single set should form parallel to the bulk shear direction. This is roughly true in the Waronga shear zone and in the Vanoise Massif, though deviation from parallelism may be as much as 20°. In the Betic Movement Zone, conjugate and alternating sets of opposite displacement suggest that late-stage deformation may have been roughly coaxial.

Acknowledgements—Many of the ideas developed in this paper arose during stimulating discussions with Gordon Lister under a variety of discouraging meteoric conditions. We are grateful to Peter Cobbold, Colin Ferguson, and Paul Williams for encouragement, advice and critical reviews. We thank Richard McAvoy, Elizabeth Orrock, and Diana Relton for technical and secretarial assistance.

REFERENCES

Berthé, D., Choukroune, P. & Jegouzo, P. 1979. Orthogneiss, mylonite, and non-coaxial deformation of granites: the example of the South Armorican Shear Zone. *J. Struct. Geol.* **1**, 31–42.

Biot, A. 1965. *Mechanics of Incremental Deformation.* Wiley, New York.

Boullier, A. M. & Gueguen, Y. 1975. SP-mylonites: origin of some mylonites by superplastic flow. *Contr. Mineral. Petrol.* **50**, 93–104.

Cobbold, P. R. 1976a. Mechanical effects of anisotropy during large finite deformations. *Bull. Soc. géol. Fr.* **18**, 1497–1510.

Cobbold, P. R. 1976b. Fold shapes as functions of progressive strain. *Phil. Trans. R. Soc.* **A283**, 129–138.

Cobbold, P. R. 1977a. Description and origin of banded deformation structures. I. Regional strain, local perturbations, and deformation bands. *Can. J. Earth Sci.* **14**, 1721–1731.

Cobbold, P. R. 1977b. Description and origin of banded deformation structures. II. Rheology and the growth of banded perturbations. *Can. J. Earth Sci.* **14**, 2510–2523.

Cobbold, P. R. 1977c. Compatibility equations and the integration of finite strain in two dimensions. *Tectonophysics* **39**, T1–T6.

Cobbold, P. R., Cosgrove, J. W. & Summers, J. M. 1971. The development of internal structures in deformed anisotropic rocks. *Tectonophysics* **12**, 23–53.

Cosgrove, J. W. 1976. The formation of crenulation cleavage. *J. geol. Soc. Lond.* **132**, 155–178.

Escher, A., Escher, J. C. & Watterson, J. 1975. The reorientation of the Kangamiut dyke swarm, West Greenland. *Can. J. Earth Sci.* **12**, 158–173.

Fletcher, R. C. 1977. Quantitative theory for metamorphic differentiation in development of crenulation cleavage. *Geology* **5**, 185–187.

Gray, D. R. 1977. Differentiation associated with discrete crenulation cleavages. *Lithos* **10**, 89–101.

Gray, D. R. 1978. Cleavages in deformed psammitic rocks from southeastern Australia: their nature and origin. *Bull. geol. Soc. Am.* **89**,

577–590.
Groshong, R. H. 1975. "Slip" cleavage caused by pressure solution in a buckle fold. *Geology* **3**, 411–413.
Hambrey, M. J. & Milnes, A. G. 1975. Boudinage in glacier ice—some examples. *J. Glaciol.* **14**, 383–393.
Hill, R. 1950. *The Mathematical Theory of Plasticity*. Oxford University Press, Oxford.
Hobbs, B. E., Means, W. D. & Williams, P. F. 1976. *An Outline of Structural Geology*. Wiley, New York.
Knill, J. L. 1959. The tectonic pattern in the Dalradian of the Craignish–Kilmelfort district, Argyllshire. *Q. Jl geol. Soc. Lond.* **115**, 339–362.
Malvern, L. E. 1969. *Introduction to the Mechanics of a Continuous Medium*. Prentice-Hall, New Jersey.
Marlow, P. C. & Etheridge, M. A. 1977. Development of a layered crenulation cleavage in mica schists of the Kanmantoo Group near Macclesfield, South Australia. *Bull. geol. Soc. Am.* **88**, 873–882.
Means, W. D. & Williams, P. F. 1972. Crenulation cleavage and faulting in an artificial salt–mica schist. *J. Geol.* **80**, 569–591.
Murrell, S. A. F. 1977. Natural faulting and the mechanics of brittle shear failure. *J. geol. Soc. Lond.* **133**, 175–190.
Nicolas, A. & Poirier, J. P. 1976. *Crystalline Plasticity and Solid State Flow in Metamorphic Rocks*. Wiley, New York.
Odé, H. 1960. Faulting as a velocity discontinuity in plastic deformation. In: *Rock Deformation* (edited by Griggs, D. J. & Handin, J.). *Mem. geol. Soc. Am.* **79**, 293–321.
Peach, B. N., Kynaston, H. & Muff, H. B. 1909. The geology of the seabord of mid-Argyll. *Mem. geol. Surv. U.K.*
Platt, J. P., Allchurch, P. D. & Rutland, R. W. R. 1978. Archaean tectonics in the Agnew supracrustal belt, Western Australia. *Precambrian Res.* **7**, 3–30.
Platt, J. P. & Lister, G. S. 1978. Déformation, métamorfisme, et mécanismes d'écoulement dans le massif de la Vanoise, Alpes penniques francaises. *C. r. hebd. Séanc. Acad. Sci., Paris* **287**, D 895–898.
Poirier, J. P. 1980. Shear localization and shear instabilities in the ductile field. *J. Struct. Geol.* **2**, 135–142.
Proffett, J. M. 1977. Cenozoic geology of the Yerington district, Nevada, and implications for the nature and origin of Basin and Range faulting. *Bull. geol. Soc. Am.* **88**, 247–266.
Ramsay, J. G. 1967. *Folding and Fracturing of Rocks*. McGraw-Hill, New York.
Ramsay, J. G. & Graham, R. 1970. Strain variation in shear belts. *Can. J. Earth Sci.* **7**, 786–813.
Rickard, M. J. 1961. A note on cleavages in crenulated rocks. *Geol. Mag.* **98**, 324–332.
Torres-Roldán, R. L. 1979. The tectonic subdivision of the Betic Zone (Betic Cordilleras, Southern Spain): its significance and one possible geotectonic scenario for the westermost Alpine belt. *Am. J. Sci.* **279**, 19–51.
Turner, F. J. & Weiss, L. E. 1963. *Structural Analysis of Metamorphic Tectonites*. McGraw-Hill, New York.
Watterson, J. 1975. Mechanism for the persistence of tectonic lineaments. *Nature, Lond.* **253**, 520–521.
White, S. H. 1976. The effects of strain on the microstructures, fabrics, and deformational mechanisms in quartzites. *Phil. Trans. R. Soc.* **A283**, 69–86.
Williams, P. F. 1972. Development of metamorphic layering and cleavage in low-grade metamorphic rocks at Bermagui, Australia. *Am. J. Sci.* **272**, 1–47.
Williams, P. F. 1976. Relationships between axial-plane foliations and strain. *Tectonophysics* **30**, 181–196.
Williams, P. F. 1979. The development of asymmetric folds in a cross-laminated siltstone. *J. Struct. Geol.* **1**, 19–30.

APPENDICES: KINEMATIC ANALYSIS

Any evolving structure is a perturbation in a flow field, and can be described in terms of spatial gradients in the rates of deformation. If the material behaves as a continuous medium, these gradients, and hence the evolution of the structure, are constrained by compatibility conditions. The effect of these constraints is examined here. For simplicity, discussion throughout is confined to constant-volume plane flow.

APPENDIX A

Compatibility conditions for flow

Flow can be expressed as the sum of a stretching-rate tensor **D**, and a vorticity tensor **W** (Malvern 1969, pp. 145–147). For two-dimensional flow in the (x, y) plane, these functions have values:

$$\mathbf{D}_{x,y} = \begin{bmatrix} \dfrac{\partial v_x}{\partial x} & \dfrac{1}{2}\left(\dfrac{\partial v_x}{\partial y} + \dfrac{\partial v_y}{\partial x}\right) \\ \dfrac{1}{2}\left(\dfrac{\partial v_x}{\partial} + \dfrac{\partial v_y}{\partial y}\right) & \dfrac{\partial v_y}{\partial y} \end{bmatrix}$$

$$\mathbf{W}_{x,y} = \begin{bmatrix} 0 & \dfrac{1}{2}\left(\dfrac{\partial v_x}{\partial y} - \dfrac{\partial v_y}{\partial x}\right) \\ \dfrac{1}{2}\left(\dfrac{\partial v_y}{\partial x} - \dfrac{\partial v_x}{\partial y}\right) & 0 \end{bmatrix} \tag{1}$$

where v_x and v_y are components of velocity parallel to the coordinate axes of a particle at the point (x, y). **D** comprises rates of elongation and shear-strain, and **W** superimposes angular velocities on these components.

For our purposes, the vorticity in two dimensions can be expressed by a single angular velocity vector **w** about the z-axis:

$$\mathbf{w}_z = \frac{1}{2}\left(\frac{\partial v_x}{\partial y} - \frac{\partial v_y}{\partial x}\right) \tag{2}$$

w is the angular velocity of a material line instantaneously parallel to the principal axes of **D**. Both **D** and **w** are functions of the velocity gradients, so their spatial variations are mutually related. These relationships constitute the flow compatibility conditions, and can be derived directly from equations (1) and (2):

$$\begin{aligned} \frac{\partial w}{\partial x} &= \frac{\partial \mathbf{D}_{xx}}{\partial y} - \frac{\partial \mathbf{D}_{xy}}{\partial x} \\ \frac{\partial w}{\partial y} &= \frac{\partial \mathbf{D}_{xy}}{\partial y} - \frac{\partial \mathbf{D}_{yy}}{\partial x} \\ \frac{\partial^2 \mathbf{D}_{xx}}{\partial y^2} + \frac{\partial^2 \mathbf{D}_{yy}}{\partial x^2} &= 2\frac{\partial^2 \mathbf{D}_{xy}}{\partial x\, \partial y}. \end{aligned} \tag{3}$$

See also Malvern (1969, p. 186), Ramsay & Graham (1970) and Cobbold (1977c).

APPENDIX B

Rotation of a perturbation

Consider a finite perturbation in a material that is otherwise undergoing homogeneous plane flow $\mathbf{D}^e$, $\mathbf{w}^e$. If a boundary is drawn that by definition completely encloses the perturbation, the volume within that boundary will experience a bulk deformation that is continuous with and identical to that of the surrounding material, even if deformation within the boundary is discontinuous and inhomogeneous. the perturbation can be treated as an element in a continuous medium, and its bulk deformation must obey the compatibility conditions.

For homogeneous plane flow,

$$\frac{\partial w}{\partial x} = \frac{\partial w}{\partial y} = 0.$$

The bulk vorticity of the perturbation ($\mathbf{w}^p$) must therefore equal $\mathbf{w}^e$. Vorticity can be expressed as the sum of two components (Lister, personal communication 1978). The vortical component ($\mathbf{w}^v$) expresses angular velocity relative to the principal axes of **D**. It is a function of the stress tensor and the rheological properties of the material. The spin component ($\mathbf{w}^s$) is the angular velocity of the principal axes of **D** relative to the chosen reference frame.

If the vortical component of flow in a perturbation is $\mathbf{w}^{pv}$, there must be a spin component $\mathbf{w}^{ps}$ to fulfil the compatibility condition, so that

$$\mathbf{w}^p = \mathbf{w}^{pv} + \mathbf{w}^{ps} = \mathbf{w}^e$$

$\mathbf{w}^{ps}$ rotates the deformational frame of the perturbation with respect to the surrounding material.

APPENDIX C

Asymmetric foliation boudinage

Asymmetric foliation boudinage comprises a shear fracture of finite length, so the structure can be treated as a finite perturbation, as in Appendix B. Assume that the material outside the perturbation

undergoes homogeneous plane flow with vorticity $\mathbf{w}^e$, using the foliation as reference frame. Inside the perturbation, assume that deformation occurs only by slip at rate Γ on the fault, initially at θ_0 to S (Fig. 4). [This can only be exactly true when the fault is at 45° to $\mathbf{D}^e_1$.] The foliation within the body (S_i) remains fixed at θ_0 to the fault. The bulk flow inside the perturbation can be described as simple shear parallel to the fault, so the fault (and hence S_i) are fixed relative to the axes of stretching rate $\mathbf{D}^p$ in the perturbation. The vortical component of flow $\mathbf{w}^{pv} = \frac{1}{2}\Gamma$. In the external reference frame, $\mathbf{w}^{ps} = \mathbf{w}^e - \mathbf{w}^{pv}$. The axes of $\mathbf{D}^p$, the fault, and S_i all rotate at $\mathbf{w}^{ps}$ relative to the foliation in the surroundings. This rotation of the entire system produces the characteristic 'reverse-drag' effect.

APPENDIX D

Spaced sets of shear-bands or faults

Consider a system of parallel shear-bands or faults spaced at intervals smaller than their length, and initially oriented at θ_0 to a set of marker lines, such as a foliation, S.

Two-dimensional coordinate axes (x, y) are defined with x parallel to the enveloping surface of the foliation (S_e). To start with, deformation occurs only by sinistral slip on the shear-bands or faults (Fig. 12). No deformation occurs between them. At a scale larger than the spacing between the bands, the material can be regarded as a continuum deforming by progressive simple shear at a rate Γ parallel to the shear-bands. This can be described by

$$\mathbf{D}_{x,y} = \begin{bmatrix} \frac{1}{2}\Gamma \sin 2\theta & \frac{1}{2}\Gamma \cos 2\theta \\ \frac{1}{2}\Gamma \cos 2\theta & -\frac{1}{2}\Gamma \sin 2\theta \end{bmatrix}$$

$$\mathbf{w}_z = \tfrac{1}{2}\Gamma \text{ anticlockwise.}$$

This deformation causes the material lines defining S_e to rotate at $\dot{\theta}$ relative to the principal axes of $\mathbf{D}$.

$$\dot{\theta} = \tfrac{1}{2}\Gamma - \tfrac{1}{2}\Gamma \cos 2\theta \text{ anticlockwise}$$

$$= \Gamma \sin^2 \theta.$$

As the principal axes of $\mathbf{D}$ in simple shear are fixed at 45° to the shear plane, this is also the angular velocity of S_e relative to the shear-bands. The shear-bands, the microlithons, and the marker lines S_i within the microlithons all rotate at $\dot{\theta}$ with respect to S_e (clockwise in Fig. 11). The angle θ between the fault and S_e decreases; the angle between S_i and S_e increases. This produces the crenulation effect in extensional crenulation cleavage. It also describes the rotation of fault-blocks in regions of extensional tectonics, such as the Basin and Range Province, Western U.S.A. (Proffett 1977).

If the bulk deformation is to conform to an externally imposed constraint some deformation will occur in the microlithons. The shear-bands and S_e will then rotate and stretch as if they were passive marker lines in a homogeneously deforming material. If the shear-bands are at ϕ to $\mathbf{D}_1$, the imposed deviatoric stretching rate is D', and the vorticity is $\mathbf{w}$, they will rotate at $\mathbf{w} \pm D' \sin 2\phi$, and stretch at $D' \cos 2\phi$. If S_e is at η to $\mathbf{D}_1$, it will rotate at $\mathbf{w} \pm D' \sin 2\eta$, and stretch at $D' \cos 2\eta$. At maximum activity, the bands will take up the entire bulk rate of shear-strain parallel to them: $2D' \sin 2\phi$. Deformation in the microlithons will then be minimal: maximum stretching-rate parallel to the bands at $D' \cos 2\phi$. This will cause S_i to rotate towards the bands at $D' \cos 2\phi \sin 2\delta$, and away from S_e at $D'(\sin 2\theta \pm \sin 2\eta - \cos 2\phi \sin 2\delta)$, where δ is the angle between S_i and the shear-bands.